Hindawi Publishing Corporation
Mathematical Problems in Engineering
Volume 2011, Article ID 187478, 19 pages
doi:10.1155/2011/187478

Research Article

Planetary Satellite Orbiters: Applications for the Moon

Jean Paulo dos Santos Carvalho,[1] Rodolpho Vilhena de Moraes,[2] and Antônio Fernando Bertachini de Almeida Prado[3]

[1] *Universidade Estadual Paulista (UNESP), 12 516-410 Guaratinguetá, SP, Brazil*
[2] *Instituto de Ciência e Tecnologia, Universidade Federal de São Paulo (UNIFESP), 12 331-280 São José dos Campos, SP, Brazil*
[3] *Division of Space Mechanics and Control, INPE, 12 227-010 São José dos Campos, SP, Brazil*

Correspondence should be addressed to Rodolpho Vilhena de Moraes, rodolpho.vilhena@gmail.com

Received 2 August 2010; Revised 9 February 2011; Accepted 17 March 2011

Academic Editor: E. E. N. Macau

Low-altitude, near-polar orbits are very desirable as science orbits for missions to planetary satellites, such as the Earth's Moon. In this paper, we present an analytical theory with numerical simulations to study the orbital motion of lunar low-altitude artificial satellite. We consider the problem of an artificial satellite perturbed by the nonuniform distribution of the mass of the Moon (J_2–J_5, J_7, and C_{22}). The conditions to get frozen orbits are presented. Using an approach that considers the single-averaged problem, we found families of periodic orbits for the problem of an orbiter travelling around the Moon, where frozen orbits valid for long periods of time are found. A comparison between the models for the zonal and tesseral harmonics coefficients is presented.

1. Introduction

Frozen orbits around the Moon, natural satellites, or asteroids are of current interest because several space missions have the goal of orbiting around such bodies (see, for instance, [1–5] and references therein). The dynamics of orbits around a planetary satellite, taking into account the gravitational attraction of a third-body and the nonuniform distribution of mass (J_2, J_3, and C_{22}) of the planetary satellite (Europa), is studied in [6–11].

This paper contains a continuation of the work developed in [1, 12, 13], where the problem of the third-body gravitational perturbation and the non-uniform distribution of mass (J_2, C_{22}) of the planetary satellite (Moon) on a spacecraft is studied using a simplified dynamical model. Also in [14, 15], the problem of critical inclination orbits for lunar artificial

Table 1: Orders of magnitude for J_2 and C_{22} [14].

	Earth	Moon
$C_{20} \equiv (-J_2)$	-10^{-3}	-2×10^{-4}
C_{22}	2×10^{-6}	2×10^{-5}

satellites including the terms (J_2) zonal, (C_{22}) sectorial, and the lunar rotation due to the lunar potential, besides the Keplerian term is considered. In [16], a study done to control the increasing eccentricity of a polar lunar satellite for different altitudes due to the perturbations of the Earth is presented. The approach presented here is the use of low-thrust propulsion in order to keep the orbital eccentricity of the satellite at low values. A fourth-order analytical theory is presented for the accurate computation of quasiperiodic frozen orbits in [17].

In our research, we use a simplified dynamical model that considers the effects caused by the nonsphericity of the Moon (J_2–J_5, J_7, and C_{22}) using single-averaged analytical model over the short satellite period. The motion of equations is obtained from the Lagrange planetary equations, and then they are integrated numerically, using the software Maple. Emphasis is given to the case of frozen orbits, defined as orbits which have constant values of eccentricity, inclination, and argument of the periapsis when the single-averaged system is considered. An approach is used for the case of frozen orbits similar to the one used in [1, 2, 5]. The basic idea is to eliminate the terms due to the short time periodic motion of the spacecraft to show smooth curves for the evolution of the mean orbital elements for a long time period. The interesting set of results allow us to find good conditions close to frozen orbits.

In other words (see [5, 11, 18, 19]), a better understanding of the physical phenomenon can be obtained and it allows the study of long-term stability of the orbits in the presence of disturbances that cause low changes in the orbital elements.

The paper has four sections. Section 2 is devoted to the terms due to the nonsphericity of the Moon and to the Hamiltonian of the system. Applications taking into account the long-period disturbing potential using the averaging method are presented in Section 3. Section 4 shows the conclusions.

2. Oblateness of the Moon

To analyze the motion of a lunar low-altitude artificial satellite, it is necessary to take into account the Moon's oblateness [1, 14, 20]. Besides that, the Moon is much less flattened than the Earth but it also causes perturbations in space vehicles. Table 1 shows the orders of magnitude for the zonal and sectorial harmonics for both celestial bodies to make a comparison. The C_{20} term describes the equatorial bulge of the Moon, often referred to as oblateness. The coefficient C_{22} measures the ellipticity of the equator.

The force function, the negative of the total energy as used in physics, is given by $F = K = V - T$ here, V is the opposite of the potential energy, and T is the kinetic energy. The force function can be written as $K = \mu/r + R - T$ or $K = \mu^2/2a + R$. The function R, comprising all terms of V except the central term, is known as the disturbing potential. The space vehicle is a point of mass in a three-dimensional orbit with orbital elements a

(semimajor axis), e (eccentricity), i (inclination), g (argument of the periapsis), h (longitude of the ascending node), and n (mean motion) given by the third Kepler law $n^2a^3 = Gm_0$, where G is the gravitational constant and r is the radius vector of the body m_0 (mass of the planetary satellite). The term due to the unperturbed potential is given by

$$H_0 = \frac{\mu^2}{2a}. \tag{2.1}$$

Considering the lunar equatorial plane as the reference plane, the disturbing potential can be written in the form [21]

$$V_M = -\frac{\mu}{r}\left[\sum_{n=2}^{5}\left(\frac{R_M}{r}\right)^n J_n P_n(\sin\phi) - \left(\frac{R_M}{r}\right)^2 C_{22}P_{22}(\sin\phi)\cos 2\lambda\right], \tag{2.2}$$

where μ is the lunar gravitational constant, R_M is the equatorial radius of the Moon (R_M = 1738 km), P_n represent the Legendre polynomials, P_{nm} represent the associated Legendre polynomials, the angle ϕ is the latitude of the orbit with respect to the equator of the Moon, and the angle λ is the longitude measured from the direction of the longest axis of the Moon, where $\lambda = \lambda' - \lambda_{22}$, since λ' is the longitude measured from any fixed direction, and λ_{22} is the longitude of the Moon's longest meridian from the same fixed direction. However, λ_{22} contains explicitly the time [20]. Using spherical trigonometry, we have $\sin(\phi) = \sin(i)\sin(f + g)$, where f is the true anomaly of the satellite.

The following assumptions will be used in this work: (a) the motion of the Moon is uniform (librations are neglected), (b) the lunar equator lies in the ecliptic (we neglect the inclination of about 1.5° of the lunar equator with respect to the ecliptic and the inclination of the lunar orbit with respect to the ecliptic of about 5°), (c) the longitude of the lunar longest meridian is equal to the mean longitude of the Earth (librations are neglected), and (d) the mean longitude of the Earth $\lambda_\oplus$ is equal to λ_{22}.

Since the variables Ω and $\lambda_\oplus$ appear only as a combination of $\Omega - \lambda_\oplus$, where $\lambda_\oplus = n_M t$ + const, n_M being the lunar mean motion. The degrees of freedom can be reduced by choosing $h = \Omega - \lambda_\oplus$ as a new variable. A new term must then be added to the Hamiltonian in order to get $\dot{h} = \dot{\Omega} - n_M = -\partial(K + n_M H)/\partial H$. This term $n_M H$ is used here in the same way it is used in [20]. The Hamiltonian is still time dependent through $\lambda_\oplus$. Since the longest meridian is always pointing toward the Earth, it is possible to choose a rotating system whose x-axis passes through this meridian.

Regarding the Earth's potential, the dominant coefficient is J_2. The rest are of higher order [2]. Opposite to the situation of the Earth, the first harmonics of the lunar potential are almost of the same order (see Table 1). This fact complicates the choice of the harmonic where the potential can be truncated, and this fact makes its choice a little arbitrary. The influences of the Earth and of the nonsphericity of the Moon on the stability of lunar satellites were also shown by [22], but the sectorial harmonics were not considered.

In terms of the orbital elements, the Legendre-associated functions for the zonal up to J_5 and sectorial (C_{22}) terms can be written in the form [20, 21]

$$\begin{aligned}
P_2(\sin\emptyset) &= \frac{1}{2}\left(3s^2\sin^2(f+g)-1\right),\\
P_3(\sin\emptyset) &= \frac{5}{2}s^3\sin^3(f+g)-\frac{3}{2}s\sin(f+g),\\
P_4(\sin\emptyset) &= \frac{35}{8}s^4\sin^4(f+g)-\frac{35}{4}s^2\sin^2(f+g)+\frac{3}{8},\\
P_5(\sin\emptyset) &= \frac{63}{8}s^5\sin^5(f+g)-\frac{35}{4}s^2\sin^3(f+g)+\frac{15}{8}s\ \sin(f+g),\\
P_{22}(\sin\emptyset)\ \cos 2\lambda &= 6\left(\xi^2\cos^2 f+x^2\sin^2 f+\xi x\ \sin 2f\right)-3\left(1-s^2\sin^2(f+g)\right),
\end{aligned} \tag{2.3}$$

where we use the shortcuts $\xi = \cos g\cos h - c\sin g\sin h$, $\chi = -\sin g\cos h - c\cos g\sin h$, $s = \sin i$, and $c = \cos i$.

With this, the zonal perturbation due to the oblateness is [14]

$$H_{20} = \epsilon\frac{\mu}{4r^3}\left(1-3c^2-3s^2\cos(2f+2g)\right), \quad \text{with } \epsilon = J_2R_M^2. \tag{2.4}$$

Replacing the relation $\mu = n^2a^3$ and using Cayley's tables [23] to express the true anomaly in terms of the mean anomaly, after some algebraic manipulations, we get

$$\begin{aligned}
H_{20} = \frac{3n^2}{8}\epsilon\Bigg[&\left(\left(5e^2-2\right)c^2+2-5e^2\right)\cos(2g+3l)+7es^2\cos(2g+3l)\\
&+17e^2s^2\cos(2g+4l)-es^2\cos(2g+l)\\
&+9\left(c^2-\frac{1}{3}\right)\left(\frac{2}{9}+\frac{2}{3}e\ \cos l+\frac{1}{3}e^2+e^2\cos 2l\right)\Bigg].
\end{aligned} \tag{2.5}$$

For the sectorial perturbation [20, 21], we get

$$H_{22} = \delta\frac{3\mu}{r^3}\left[2\xi^2\cos^2 f+2\chi^2\sin^2 f+2\xi\chi\sin 2f-1+s^2\sin^2(f+g)\right], \tag{2.6}$$

where $\delta = C_{22}R_M^2$. With some manipulations, we get

$$\begin{aligned}
H_{22} = -\frac{45}{16}\delta n^2 \Bigg[& \left(e^2 - \frac{2}{5}\right)(c-1)^2 \cos(2l + 2g - 2h) \\
& - \frac{1}{3}(c+1)^2\left(e^2 - \frac{2}{5}\right)\cos(2l - 2g - 2h) + (c+1)^2\left(e^2 - \frac{2}{5}\right)\cos(2l + 2g + 2h) \\
& - \frac{1}{3}\left(e^2 - \frac{2}{5}\right)(c-1)^2 \cos(2l - 2g + 2h) - \frac{17}{5}e^2(c-1)^2 \cos(4l + 2g - 2h) \\
& - \frac{7}{5}e(c-1)^2 \cos(3l + 2g - 2h) + \frac{17}{15}e^2(c+1)^2 \cos(4l - 2g - 2h) \\
& + \frac{7}{15}e(c+1)^2 \cos(3l - 2g - 2h) - \frac{7}{5}e(c+1)^2 \cos(3l + 2g + 2h) \\
& - \frac{17}{5}e^2(c+1)^2 \cos(4l + 2g + 2h) + \frac{7}{15}e(c-1)^2 \cos(3l - 2g + 2h) \\
& + \frac{17}{15}e^2(c-1)^2 \cos(4l - 2g + 2h) - \frac{1}{15}e(c+1)^2 \cos(l - 2g - 2h) \\
& + \frac{1}{5}e(c-1)^2 \cos(l + 2g - 2h)\frac{1}{5}e(c+1)^2 \cos(l + 2g + 2h) \\
& - \frac{1}{15}e(c-1)^2 \cos(l - 2g + 2h) - \frac{2}{3}s^2\left(e^2 - \frac{2}{5}\right)\cos(2l - 2g) \\
& + \frac{9}{5}e^2 \cos(2l - 2h) - \frac{7}{5}e\cos(3l - 2g) + \frac{1}{5}e\cos(l - 2g) \\
& + \frac{9}{5}e^2 \cos(2l + 2h) + \frac{2}{5}\left(3e^2 + 2\right)\cos 2h - \frac{17}{5}e^2 \cos(4l - 2g) \\
& + \frac{6}{5}e\cos(l + 2h) + \frac{6}{5}e\cos(l - 2h)\Bigg],
\end{aligned} \tag{2.7}$$

where the disturbing potential is written in the form $R = H_{20} + H_{22}$.

2.1. The Hamiltonian System

The Hamiltonian of the dynamical system associated with the problem of the orbital motion of the satellite around the Moon taking into account the non-uniform distribution of the mass of the planetary satellite (J_2–J_5, J_7, and C_{22}) can be written in the following form:

$$K = H_0 + \sum_{i=2}^{5} H_{i0} + H_{70} + H_{22}, \tag{2.8}$$

where

$$H_0 = \frac{\mu^2}{2a} + n_M H. \tag{2.9}$$

Now, using $\sum_{i=1}^{4} H_{(i+1)0} = \sum_{i=1}^{4} \epsilon_i H_i$, $H_{70} = \epsilon_5 H_5$ and $H_{22} = \delta H_6$, we get

$$K = H_0 + \sum_{i=1}^{5} \epsilon_i H_i + \delta H_6, \tag{2.10}$$

where $\epsilon_1 = J_2 R_M^2$, $\epsilon_2 = J_3 R_M^3$, $\epsilon_3 = J_4 R_M^4$, $\epsilon_4 = J_5 R_M^5$, $\epsilon_5 = J_7 R_M^7$, $\delta = C_{22} R_M^2$.

We arrange the Hamiltonian K as follows

$$K = H_0^0 + H_1^1, \tag{2.11}$$

where

$$H_0^0 = \frac{\mu^2}{2a} + n_M H, \tag{2.12}$$

$$H_1^1 = \sum_{i=1}^{5} \epsilon_i H_i + \delta H_6. \tag{2.13}$$

The motion of the spacecraft is studied under the single-averaged analytical model. The average is taken over the mean motion of the satellite. The standard definition for average used in this research is [24] $\langle F \rangle = 1/2\pi \int_0^{2\pi} (F) dl$ where l is the mean anomaly of the satellite. The single-average method is applied in (2.13) to eliminate the terms of short period, to analyze the effect of the disturbing potential on the orbital elements. Periodic terms will be calculated, replacing the result in the Lagrange planetary equations [25] and numerically integrated using the Maple software. The long-period disturbing potential is given in the appendix.

3. Applications: The Long-Period Disturbing Potential Using the Averaging Method

With a simplified model for the disturbing potential, it is possible to analyse the orbital motion of the satellite.

To study the lifetimes of low-altitude artificial satellites of the Moon [26] we took into account the zonal (J–J_5) and sectorial (C_{22}, C_{31}) terms in the disturbing potential. However, [5] shows that the effect of the J_7 term is an order of magnitude larger than the J_2–J_5 terms (see Table 2, model given by [27]), and therefore it should be considered in the potential. In [5], an analytic model is presented to find frozen orbits for lunar satellites, where the potential only due to J_2 and J_7 zonal harmonics is taken into account. In this paper, we present an approach taking into account the J_2–J_5, J_7, and C_{22} terms.

Table 2: Coefficients given by [27].

Coefficients	
J_2	$+2.070 \times 10^{-4}$
J_3	$+4.900 \times 10^{-6}$
J_4	$+8.000 \times 10^{-7}$
J_5	-3.600×10^{-6}
J_6	-1.100×10^{-6}
J_7	-2.870×10^{-5}
C_{22}	$+2.447305 \times 10^{-5}$

Table 3: Model given by [28] (LP165P).

Coefficients [29]	
J_2	$+2.032337 \times 10^{-4}$
J_3	$+8.475900 \times 10^{-6}$
J_4	-9.591930×10^{-6}
J_5	$+7.154090 \times 10^{-7}$
J_6	-1.357770×10^{-5}
J_7	-2.177470×10^{-5}
J_8	-9.674870×10^{-6}
J_9	$+1.549600 \times 10^{-5}$
C_{22}	$+2.235700 \times 10^{-5}$

3.1. Frozen Orbits Solutions

The definition of frozen orbit is written in the form

$$\frac{dg}{dt} = 0, \qquad \frac{de}{dt} = 0, \qquad \frac{di}{dt} = 0. \tag{3.1}$$

From this, we can obtain frozen orbits, say, for $g = \pi/2$ or $g = 3\pi/2$, and $h = \pi/2$ or $h = 3\pi/2$ (see [1, 13]).

Replacing by the potential in (A.1) in the Lagrange's planetary equations [25] and solving the equation $dg/dt = 0$, we get an equation that depends on three variables, e, i, and a, that can be represented as a 3-D surface as shown in Figures 1, 2, 3, and 4. Points on this surface correspond to equilibria of the system in equations $dg/dt = 0$ and $de/dt = 0$, that is, frozen orbits. Figures 1 and 3 take into account the coefficients J_2–J_5 and J_7, while Figures 2 and 4 take into account the J_2–J_5, J_7, and C_{22} terms. Comparing the models given by [27] (see Table 2) and [28] (see Table 3), we can analyze that the results are very close and the model given by [28] presents better results to obtain a family of frozen orbits for inclinations above 69°. In [30], an analytical theory based on Lie-Deprit transformation is used to locate family of frozen orbits for asteroids and natural satellites.

For inclinations larger than 69°, we found a family of frozen orbit, as we can see in Figures 1, 2, 3, and 4, mainly considering the model LP165P for the coefficients of the lunar gravity field [28]. We also observed that the C_{22} term contributed efficiently to obtain of such orbits.

The curves obtained for constant-a sections are very similar; thus, in order to go into more detail, we define a constant value for the semimajor axis $a = 1861$ km, which indeed

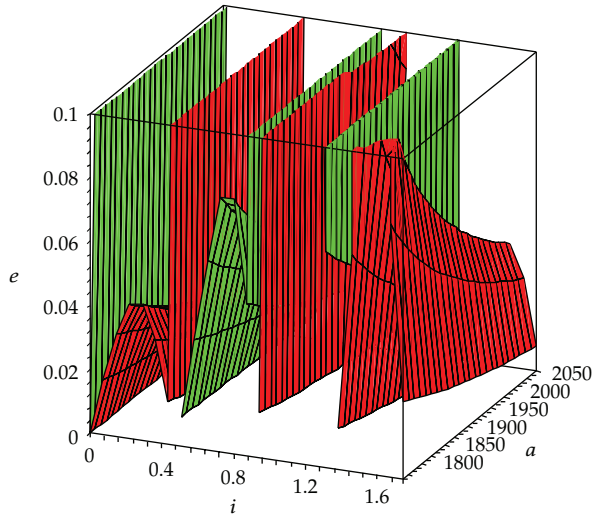

Figure 1: e versus i-rad versus a-km. Akim, [27], J_2–J_5, J_7. Green color is the surface when $g = 3\pi/2$, and the red is obtained for $g = \pi/2$.

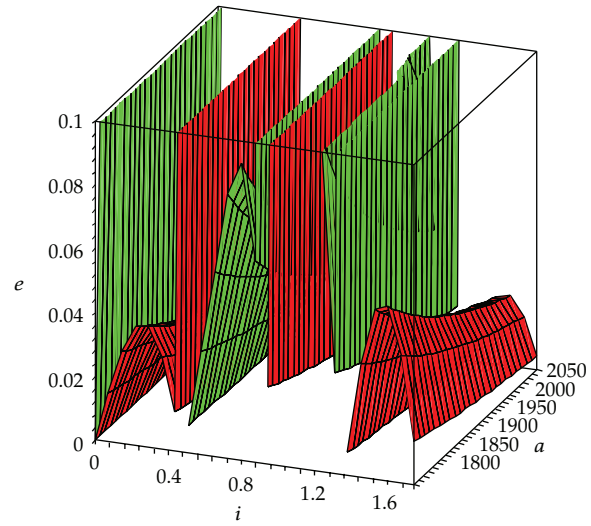

Figure 2: e versus i-rad versus a-km. Akim, [27], J_2–J_5, J_7 and C_{22}. Green color is the surface when $g = 3\pi/2$, and the red is obtained for $g = \pi/2$.

corresponds to low orbits. For the chosen value of a, we plot the curve i versus e (see Figures 5 and 6). Figure 5 does not take into account the C_{22} term in the potential, while Figure 6 considers the sectorial term. We observed an increase of the eccentricity for inclinations between 28.65° and 45.84° (comparing Figures 5 and 6). For orbits with inclination larger than 69° degree, we find a family of frozen orbits (see Figure 6). The region where the eccentricity is frozen is for small values of the initial eccentricity, when compared with Figure 5.

Taking into account that Figure 6 represents a family of frozen orbits for inclinations of 90°, an example to illustrate the behavior of the frozen orbits for a case where the semimajor

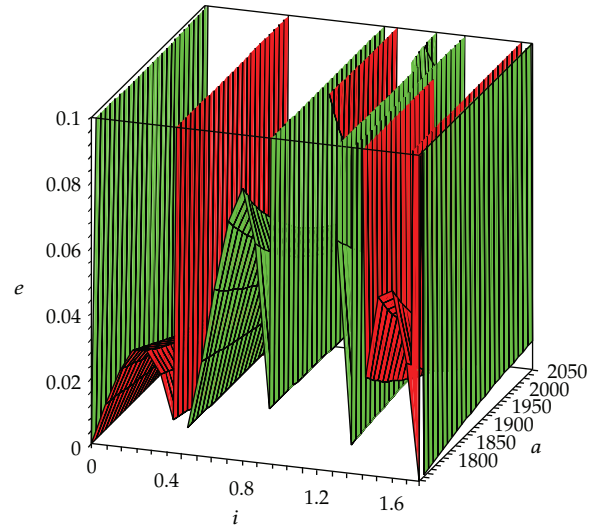

Figure 3: e versus i-rad versus a-km. LP165P, Konopliv et al. [28], J_2–J_5, J_7. Green color is the surface when $g = 3\pi/2$, and the red is obtained for $g = \pi/2$.

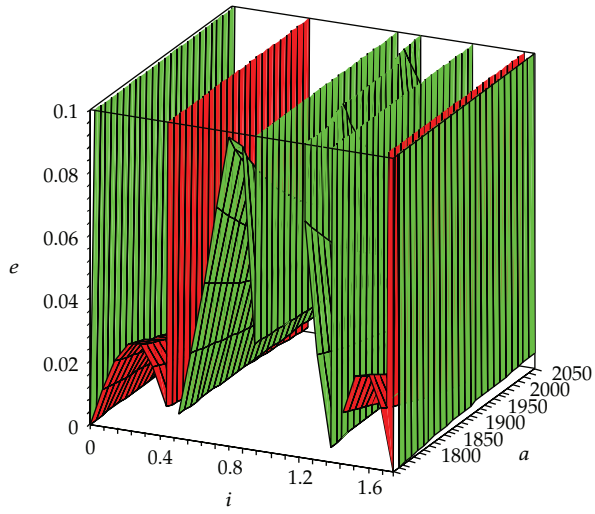

Figure 4: e versus i-rad versus a-km. LP165P, Konopliv et al. [28], J_2–J_5, J_7 and C_{22}. Green color is the surface when $g = 3\pi/2$, and the red is obtained for $g = \pi/2$.

axis is 1861 km is shown in Figures 7, 9, and 10. Figures 7–10 are obtained by numerical integration (using the software Maple) of the Lagrange planetary equations for different values of the eccentricity. Figure 8 shows frozen orbits for a case where the semimajor axis is 1838 km.

We found frozen orbits with initial eccentricity equal to 0.02 that can be applied for missions of long period without the needs for doing orbit corrections for a period of very long time (larger than 4000 days). The initial orbit with appropriate characteristics can extend

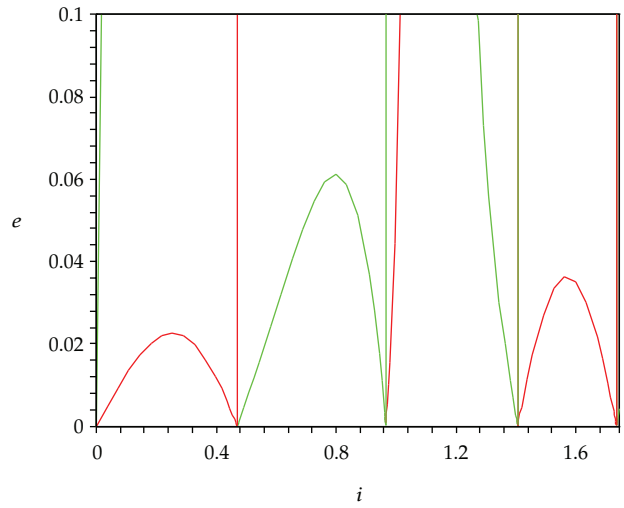

Figure 5: e versus i-rad, $a = 1861$ km. LP165P, Konopliv et al. [28], J_2–J_5 and J_7. Green color is obtained for $g = 3\pi/2$, and the red is obtained for $g = \pi/2$.

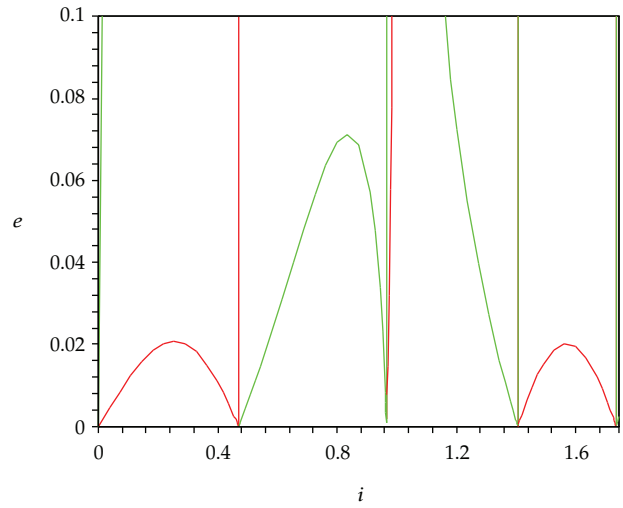

Figure 6: e versus i-rad, $a = 1861$ km. LP165P, Konopliv et al. [28], J_2–J_5, J_7, and C_{22}. Green color is obtained for $g = 3\pi/2$, and the red is obtained for $g = \pi/2$.

the time life and reduce maintenance costs. The set of initial conditions for frozen orbits with long lifetime is given by $a = 1861$ km, $e = 0.02$, $i = 90°$, $g = 90°$, and $h = 270°$.

In the literature, in general, frozen polar orbits are found with periapsis $g = 270°$ [3, 31–33], however, for orbits with inclinations near 90°, the argument of periapsis moves to $g = 90°$ [2, 31, 34]. These authors take into account only the zonal terms. In [34], there is an approach that compares the disturbing potential when a model of the gravitational field of high order taking into account the terms J_7, J_{20}, and J_{50} is considered. For small inclinations, the three models show similar results for low-altitude orbits (see [34]), while for high inclination orbits the J_{20} truncation only approximates roughly the J_{50} case, giving frozen orbits that, in general,

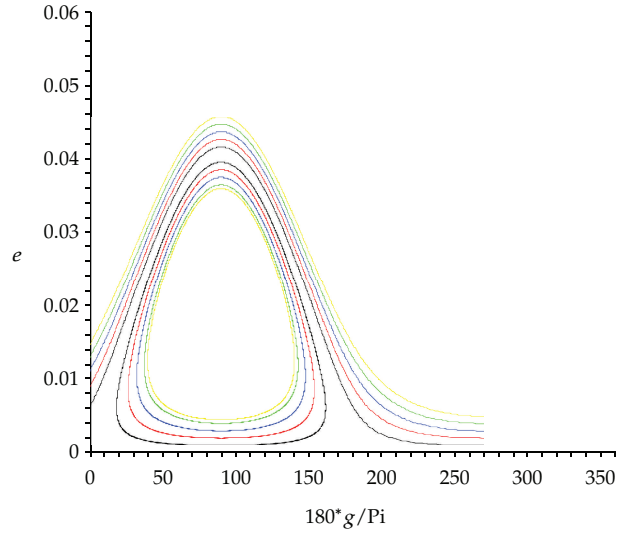

Figure 7: e versus g-degree. Model LP165P. Initial conditions: $i = 90°$, $a = 1861$ km, $e = 0.001$, black color; $e = 0.002$, red color; $e = 0.003$, blue color; $e = 0.004$ green color. Perturbations: J_2–J_5, J_7, and C_{22}.

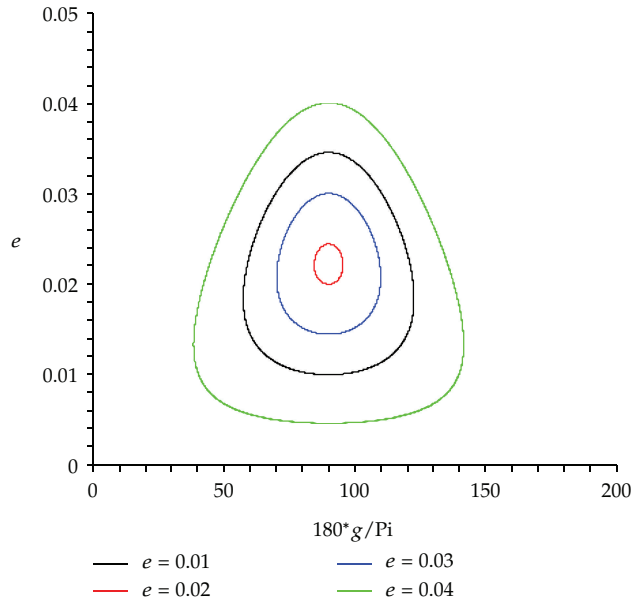

Figure 8: e versus g-degree. Model LP165P. Initial conditions: $i = 90°$, $a = 1838$ km. Perturbations: J_2–J_5, J_7, and C_{22}.

show lower eccentricities and shifting the zero eccentricity solutions to lower inclinations by several degrees. In this case, the potential truncated in the J_7 term provides a qualitative description only correct in the case of low inclinations. In [35], a numerical study considering models for the lunar gravity field of high order is applied to near-circular, low-altitude orbits. The behavior of the periapsis altitude is analyzed for some harmonics, for example, J_7 and J_9.

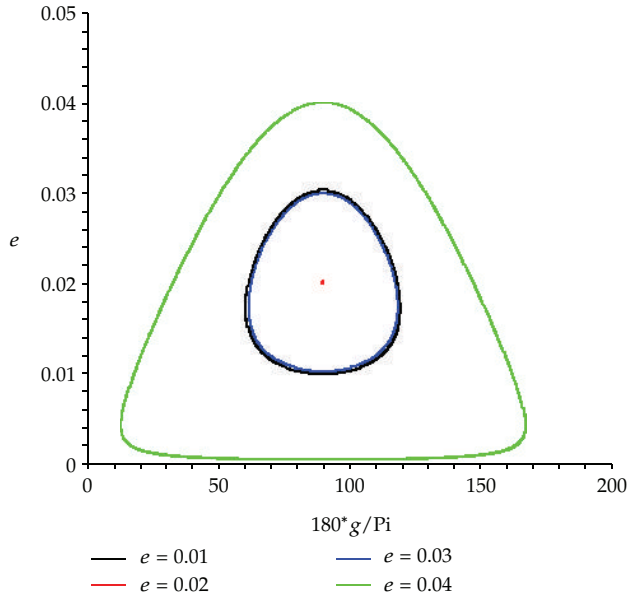

Figure 9: e versus g-degree. Model LP165P. Initial conditions: $i = 90°$, $a = 1861$ km. Perturbations: J_2–J_5, J_7, and C_{22}.

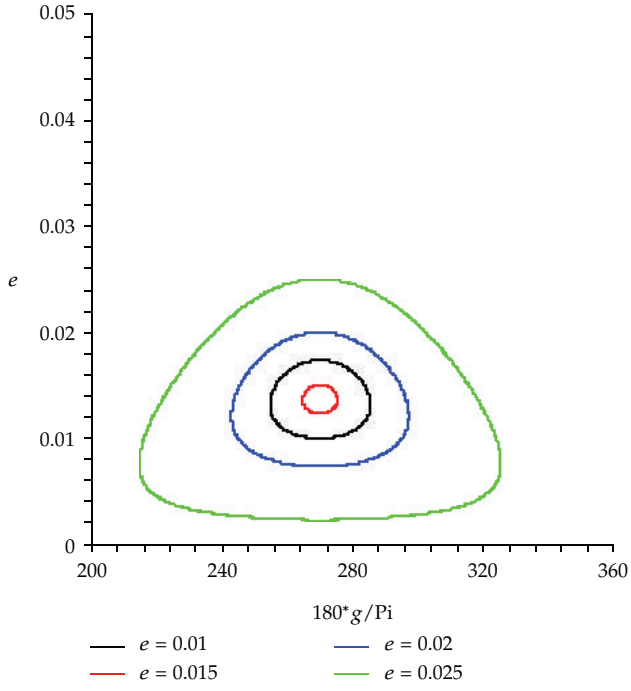

Figure 10: e versus g-degree. Model LP165P. Initial conditions: $i = 90°$, $a = 1861$ km. Perturbations: J_2–J_5 and C_{22}.

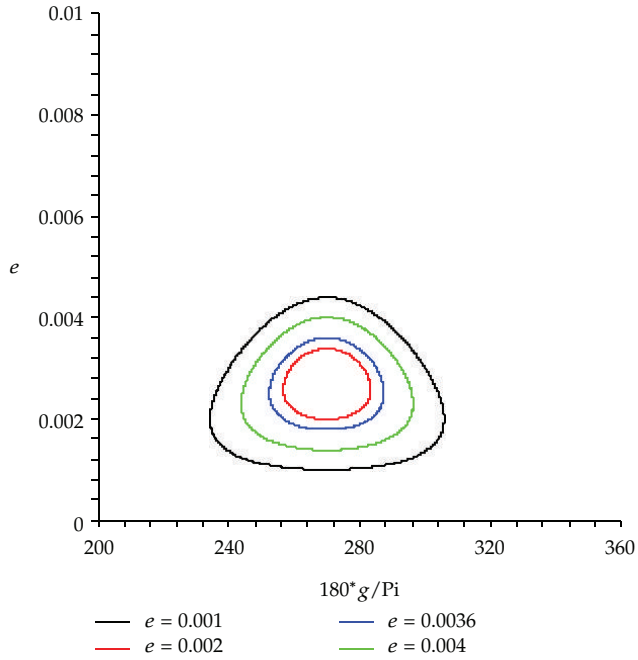

Figure 11: e versus g-degree. Model LP165P. Initial conditions: $i = 90°$, $a = 1861$ km. Perturbations: J_2–J_9 and C_{22}.

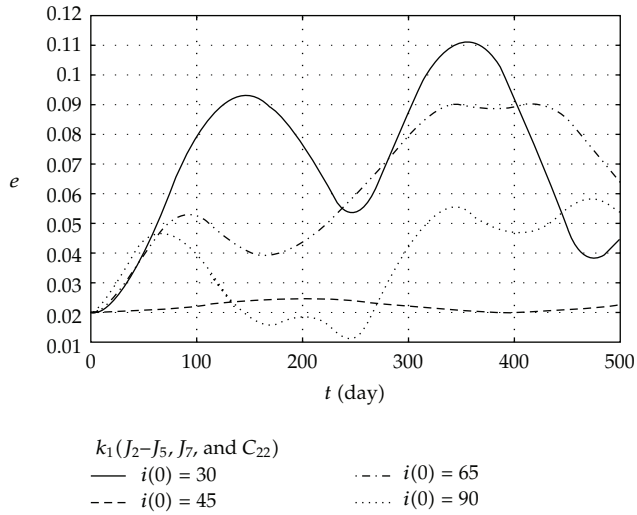

Figure 12: LP165P Model, $e = 0.02$, $g = 90°$, and $h = 270°$.

Here, we truncate the potential of the lunar gravity field up to the J_7 term, to analyze the effect caused by this harmonic in particular [5]. When we consider the potential taking into account the terms J_2–J_5 and C_{22} (zonal and sectorial), the frozen orbit ($i = 90°$, see Figure 10) librates around the equilibrium point for $g = 270°$ which is in agreement with the literature (see [3, 31, 32]). But, when we take into account the potential up to the J_7

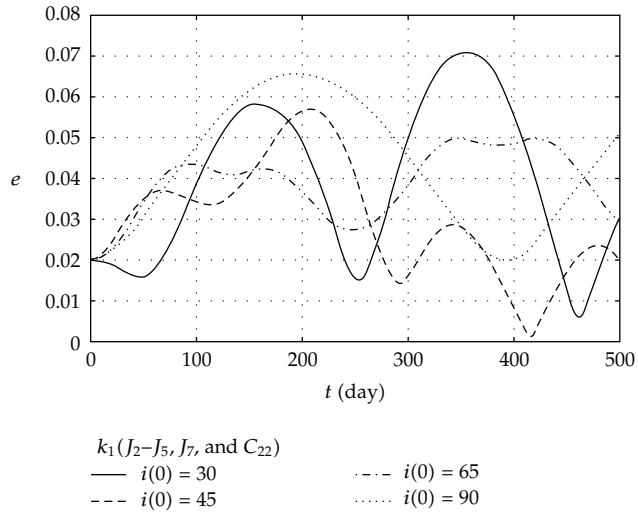

Figure 13: LP165P Model, $e = 0.02$, $g = 270°$, and $h = 90°$.

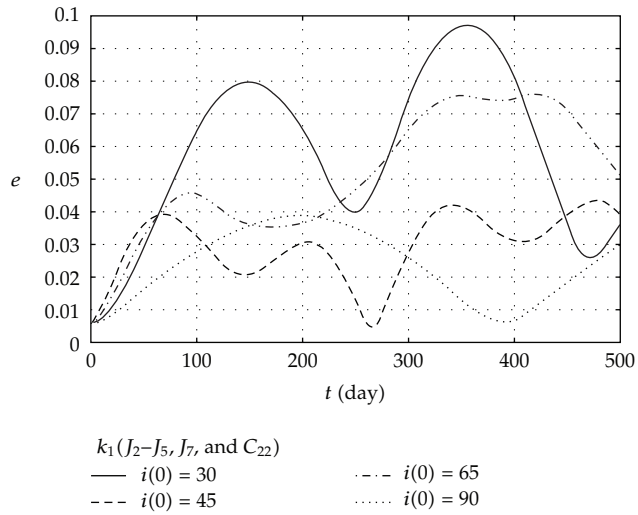

Figure 14: LP165P Model, $e = 0.006$, $g = 90°$, and $h = 270°$.

term, we found frozen orbits that librate around the equilibrium point for $g = 90°$, which is in agreement with [5]. In [34], a frozen orbit considering the following initial conditions: $a = 1861$ km, $e = 0.0036$, $i = 84°$, and $g = 90°$, is found, and it corresponds to a near-polar orbit.

Then, we develop the disturbing potential up to the J_9 term (J_2–J_9, C_{22}) to analyze what happens with the value of g for a low-altitude, near-circular, near-polar orbit. Figure 11 shows the behavior for the diagram e versus g for a polar orbit which librates around the equilibrium point for the value of $g = 270°$ (see [33] for more details with respect to the potential truncated up to the J_9 term.). In this case, the initial eccentricity varies from 0.001 to 0.004. The numerical values used for the harmonics up to J_9 is given in Table 3. Thus, we conclude that, because of the characteristics of the lunar gravity field, the potential truncated

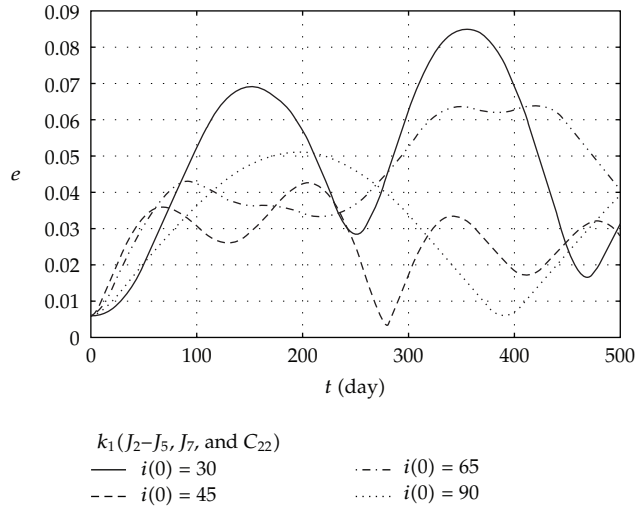

Figure 15: LP165P Model, $e = 0.006$, $g = 270°$, and $h = 90°$.

up to the J_7 produces the effect of the frozen orbit obtained that librates around $g = 90°$ and not $g = 270°$.

The idea here is to consider a simplified potential to analyze the effect of the harmonics on the orbital elements e and g. Therefore, this study did not realize the full potential integrations, which can be viewed in [33, 34].

Another important factor that we must analyze is the value of the argument of the periapsis, that strongly affects the determination of the frozen orbit. As we previously showed, the values of the periapsis to assure the condition of frozen orbit are $g = 90°$ or $g = 270°$, equally for the longitude of the ascending node that is $h = 90°$ or $h = 270°$. Since that, in general, we find frozen orbits for the value of $g = 90°$. Figures 12–15 show the behavior of the eccentricity as a function of time for different values of the inclinations. Note that Figure 12 presents an orbit with lesser variation of the eccentricity for inclination of $i = 90°$, considering $g = 90°$. When we compare Figure 12 with Figure 13, we get that, for the value of $g = 270°$, the orbit presents great variations of the eccentricity. We also analyze the case for the initial eccentricity of the order of 10^{-3} and verify that the behavior of the orbit does not suffer the same effect as occurred for the case of the eccentricity of order 10^{-2}. Here, the value of $g = 90°$ or $g = 270°$ has smaller effect on the amplitude of the eccentricity (see Figures 14 and 15).

4. Conclusions

In this paper, the dynamics of orbits around a planetary satellite (Moon), taking into account the non-uniform distribution of mass (J_2–J_9 and C_{22}), was studied. Several analyses were performed, using the long-period disturbing potential obtained through the single-averaged model.

Considering the long-period disturbing potential, we found a family of frozen orbits for inclinations larger than 69° considering the model LP165P for the coefficients of the lunar gravity field. It was observed that the C_{22} term contributed efficiently to obtain such orbits.

Low-altitude, near-polar orbits are very desirable for scientific missions to study natural satellites, such as the Moon. Due to the characteristics of the lunar gravity field, the potential truncated up to the J_7 produces the effect of the frozen orbit that librates around $g = 90°$ and not $g = 270°$. Considering the long-period disturbing potential using the single-averaged method, we found near-circular, near-polar frozen orbits where this choice reduces the maintenance cost considerably.

In general, we conclude that, for the case of the Moon, it is necessary to consider a gravity model of high order, including the zonal and sectorial terms. Because the question of the coefficients are almost of the same order, this fact complicates the choice of the harmonic where the potential can be truncated and fact makes its choice a little arbitrary.

To study the lifetime of a lunar artificial satellite considering an analytical model, the zonal (J_2–J_9) and sectorial (C_{22}) terms of the harmonic coefficients should be taken into account. We observe that the frozen orbits could be strongly affected by terms of the potential containing the coefficient due to the equatorial ellipticity of the Moon (C_{22}) and by terms containing the argument of the periapsis and the longitude of the ascending node.

Appendix

The long-period disturbing potential up to the J_7 term is

$$
\begin{aligned}
k1 \quad = \frac{75}{16a^5}\, n^2 \Bigg(& -\frac{8807799}{163840} \\
& \times \Bigg(-\frac{130330}{38129}c^2 + \frac{31545}{38129} + c^4\epsilon_4 e^4 \\
& + \Bigg(-\frac{11136}{14665}\epsilon_4 c^4 + \Bigg(\frac{18432}{419419}a^2\epsilon_3 + \frac{12928}{27235}\epsilon_4 \Bigg) c^2 \\
& - \frac{94208}{3774771}a^2\epsilon_3 - \frac{104448}{2097095}\epsilon_4 \Bigg) \\
& \times e^2 - \frac{256}{2933}\epsilon_4 c^4 + \Bigg(\frac{2048}{419419}a^2\epsilon_3 + \frac{1536}{38129}\epsilon_4 \Bigg) c^2 \\
& - \frac{2048}{3774771}a^2\epsilon_3 - \frac{768}{419419}\epsilon_4 \Bigg) s^3 e^3 \sin(3g) + \frac{10731721}{1474560}s^5 \\
& \times \Bigg(\epsilon_4 \Bigg(-\frac{1178377}{696865} + c^2 \Bigg) e^2 + \frac{114912}{696865}\epsilon_4 - \frac{6624}{53605}\epsilon_4 c^2 - \frac{36864}{7665515}a^2\epsilon_3 \Bigg) \\
& \times e^5 \sin(5g) - \frac{49}{40}\left(e^2 + \frac{2}{7}\right)\epsilon_2 \left(c^2 - \frac{1}{7}\right) a^3 s^2 e^2 \cos(2g) \\
& + \frac{12}{25}\,\delta\, a^5 s^2 \left(e^2 + \frac{2}{3}\right)\cos(2h) + \frac{54197}{294912}\,\epsilon_4 s^7 e^7 \sin(7g) \\
& + \frac{2381620241}{1474560}\left(c^6 - \frac{40098159}{30930133}c^4 - \frac{33943925}{1020694389} + \frac{13741935}{30930133}c^2\right)\epsilon_4\, e^6
\end{aligned}
$$

$$
\begin{aligned}
&+\left(\frac{1964963}{5120}\ \epsilon_4 c^6+\left(-\frac{5173}{160}a^2\epsilon_3-\frac{2256793}{5120}\ \epsilon_4\right)c^4\right.\\
&\quad\left.+\left(\frac{121765}{1024}\ \epsilon_4+\frac{2527}{120}\ a^2\epsilon_3\right)c^2-\frac{637}{480}\ a^2\epsilon_3-\frac{4263}{1024}\ \epsilon_4\right)e^4\\
&+\left(\frac{27027}{320}\ \epsilon_4\ c^6+\left(-\frac{441}{40}\ a^2\epsilon_3-\frac{6237}{64}\ \epsilon_4\right)c^4+\right.\\
&\quad\left.\times\left(\frac{147}{20}\ a^2\epsilon_3+\frac{1701}{64}\ \epsilon_4+\epsilon_1\ a^4\right)c^2-\frac{21}{40}\ a^2\epsilon_3-\frac{1}{5}\ \epsilon_1\ a^4-\frac{63}{64}\ \epsilon_4\right)\\
&\times e^2+\frac{3003}{320}\ \epsilon_4\ c^6+\left(-\frac{21}{10}\ a^2\epsilon_3-\frac{693}{64}\ \epsilon_4\right)c^4\\
&+\left(\frac{189}{64}\ \epsilon_4+\frac{2}{5}\epsilon_1\ a^4+\frac{7}{5}a^2\epsilon_3\right)c^2-\frac{2}{25}\ \epsilon_1\ a^4\\
&\left.-\frac{7}{64}\ \epsilon_4-\frac{1}{10}\ a^2\epsilon_3\right)se\ \sin(g)-\frac{147}{32}\\
&\times\left(\left(c^4-\frac{6}{7}c^2+\frac{3}{35}\right)\epsilon_2\ e^4\right.\\
&+\left(\frac{8}{21}\ \epsilon_2\ c^4+\left(-\frac{64}{1225}\ a^2\epsilon-\frac{16}{49}\ \epsilon_2\right)c^2+\frac{64}{3675}\ a^2\epsilon+\frac{8}{245}\ \epsilon_2\right)\\
&\left.\times e^2+\frac{8}{105}\ \epsilon_2\ c^4+\left(-\frac{16}{245}\ \epsilon_2-\frac{128}{3675}\ a^2\epsilon\right)c^2+\frac{128}{11025}\ a^2\epsilon+\frac{8}{1225}\ \epsilon_2\right)a^3\Bigg),
\end{aligned}
\tag{A.1}
$$

where the values for the zonal (J_2–J_7) and tesseral (C_{22}) harmonics coefficients taking into account the two models are given in Table 2 [27] and Table 3 [28].

Acknowledgment

This work was accomplished with the support of the FAPESP under the contract no. 2007/04413-7 and 2006/04997-6, SP-Brazil, and CNPQ (300952/2008-2).

References

[1] J. P. S. Carvalho, R. Vilhena de Moraes, and A. F. B. A. Prado, "Some orbital characteristics of lunar artificial satellites," *Celestial Mechanics & Dynamical Astronomy*, vol. 108, no. 4, pp. 371–388, 2010.

[2] A. Elipe and M. Lara, "Frozen orbits about moon," *Journal of Guidance, Control and Dynamics*, vol. 26, no. 2, pp. 238–243, 2003.

[3] D. Folta and D. Quinn, "Lunar frozen orbits," Paper AIAA 2006-6749, August 2006.

[4] S. Y. Park and J. L. Junkins, "Orbital mission analysis for a lunar mapping satellite," *Journal of the Astronautical Sciences*, vol. 43, no. 2, pp. 207–217, 1995.

[5] A. Abad, A. Elipe, and E. Tresaco, "Analytical model to find frozen orbits for a lunar orbiter," *Journal of Guidance, Control, and Dynamics*, vol. 32, no. 3, pp. 888–898, 2009.

[6] D. J. Scheeres, M. D. Guman, and B. F. Villac, "Stability analysis of planetary satellite orbiters: application to the Europa orbiter," *Journal of Guidance, Control, and Dynamics*, vol. 24, no. 4, pp. 778–787, 2001.

[7] M. Lara and J. F. S. Juan, "Dynamic behavior of an orbiter around Europa," *Journal of Guidance, Control, and Dynamics*, vol. 28, no. 2, pp. 291–297, 2005.

[8] M. Lara, "Simplified equations for computing science orbits around planetary satellites," *Journal of Guidance, Control, and Dynamics*, vol. 31, no. 1, pp. 172–181, 2008.

[9] M. E. Paskowitz and D. J. Scheeres, "Design of science orbits about planetary satellites: application to Europa," *Journal of Guidance, Control, and Dynamics*, vol. 29, no. 5, pp. 1147–1158, 2006.

[10] J. P. S. Carvalho, A. Elipe, R. Vilhena de Moraes, and A. F. B. A. Prado, "Frozen Orbits around the Europa Satellite," in *Proceedings of the International Conference on Chaos and Nonlinear Dynamics*, Dynamics Days South America 2010, INPE, São José dos Campos, Brazil, July 2010.

[11] M. Lara, J. F. Palacián, and R. P. Russell, "Mission design through averaging of perturbed Keplerian systems: the paradigm of an Enceladus orbiter," *Celestial Mechanics and Dynamical Astronomy*, vol. 108, no. 1, pp. 1–22, 2010.

[12] J. P. S. Carvalho, A. Elipe, R. Vilhena de Moraes, and A. F. B. A. Prado, "Moon artificial satellites: lunar oblateness and earth perturbations," in *Proceedings of the International Conference on Nonlinear Problems in Aviation and Aerospace (ICNPAA '09)*, pp. 1095–1106, Cambrige Scientific, Genoa, Italy, 2009.

[13] J. P. S. Carvalho, A. Elipe, R. Vilhena de Moraes, and A. F. B. A. Prado, "Nonsphericity of the moon and near sun-synchronous polar lunar orbits," *Mathematical Problems in Engineering*, vol. 2009, pp. 1–25, 2009.

[14] B. De Saedeleer, "Analytical theory of a lunar artificial satellite with third body perturbations," *Celestial Mechanics & Dynamical Astronomy*, vol. 95, no. 1–4, pp. 407–423, 2006.

[15] S. Tzirti, K. Tsiganis, and H. Varvoglis, "Quasi-critical orbits for artificial lunar satellites," *Celestial Mechanics & Dynamical Astronomy*, vol. 104, no. 3, pp. 227–239, 2009.

[16] O. C. Winter, D. C. Mourão, C. F. Melo, E. N. Macau, J. L. Ferreira, and J. P. S. Carvalho, "Controlling the eccentricity of polar lunar orbits with low-thrust propulsion," *Mathematical Problems in Engineering*, vol. 2009, Article ID 159287, 10 pages, 2009.

[17] M. Lara and J. F. Palacián, "Hill problem analytical theory to the order four: application to the computation of frozen orbits around planetary satellites," *Mathematical Problems in Engineering*, vol. 2009, Article ID 753653, 18 pages, 2009.

[18] S. Ferrer, J. F. San-Juan, and A. Abad, "A note on lower bounds for relative equilibria in the main problem of artificial satellite theory," *Celestial Mechanics & Dynamical Astronomy*, vol. 99, no. 1, pp. 69–83, 2007.

[19] J. F. Palacián, "Dynamics of a satellite orbiting a planet with an inhomogeneous gravitational field," *Celestial Mechanics & Dynamical Astronomy*, vol. 98, no. 4, pp. 219–249, 2007.

[20] G. E. O. Giacaglia, J. P. Murphy, and T. L. Felsentreger, "A semi-analytic theory for the motion of a lunar satellite," *Celestial Mechanics*, vol. 3, no. 1, pp. 3–66, 1970.

[21] M. Radwan, "Analytical approach to the motion of a lunar artificial satellite," *Astrophysics and Space Science*, vol. 283, no. 2, pp. 133–150, 2003.

[22] Z. Knežević and A. Milani, "Orbit maintenance of a lunar polar orbiter," *Planetary and Space Science*, vol. 46, no. 11-12, pp. 1605–1611, 1998.

[23] A. Cayley, "Tables of the developments of functions in theory of elliptic motion," *Memoirs of the Royal Astronomical Society*, vol. 29, pp. 191–306, 1861.

[24] V. G. Szebehely, *Adventures in Celestial Mechanics*, University of Texas Press, Austin, Tex, USA, 1989.

[25] J. Kovalevsky, *Introduction to Celestial Mechanics*, Bureau des Longitudes, Paris, France, 1967.

[26] W. K. Meyer, J. J. Buglia, and P. N. Desai, "Lifetimes of lunar satellite orbits," Tech. Rep. N-TP-3394 94, 27771, NASA STI/Recon, 1994.

[27] E. Akim, "Determination of the gravity field of the moon from movement of artificial satellite of the moon luna-10," *Doklady Akademii Nauk USSR*, vol. 170, no. 4, pp. 799–802, 1966.

[28] A. S. Konopliv, S. W. Asmar, E. Carranza, W. L. Sjogren, and D. N. Yuan, "Recent gravity models as a result of the Lunar Prospector mission," *Icarus*, vol. 150, no. 1, pp. 1–8, 2001.

[29] J.-Y. Chen, J.-S. Ning, C.-Y. Zhang, and J. Lou, "On the determination of lunar gravity field in the Chinese first lunar prospector mission," *Chinese Journal of Geophysics*, vol. 48, no. 2, pp. 275–281, 2005.

[30] J. F. San-Juan, "Analytical model for lunar orbiter revisited," *Advances in the Astronautical Sciences*, vol. 136, pp. 245–263, 2010.

[31] L. Lin and W. Hai-hong, "Two problems about the motion of low-moon-orbit satellites," *Chinese Astronomy and Astrophysics*, vol. 30, no. 4, pp. 437–446, 2006.

[32] R. P. Russell and M. Lara, "Long-lifetime lunar repeat ground track orbits," *Journal of Guidance, Control, and Dynamics*, vol. 30, no. 4, pp. 982–993, 2007.
[33] M. Lara, S. Ferrer, and B. De Saedeleer, "Lunar analytical theory for polar orbits in a 50-degree zonal model," *Advances in the Astronautical Sciences*, vol. 134, pp. 881–897, 2009.
[34] M. Lara, B. De Saedeleer, and S. Ferrer, "Preliminary design of low lunar orbits," in *Proceedings of the 21st International Symposium on Space Flight Dynamics*, pp. 1–15, Toulouse, France, 2009.
[35] R. V. Ramanan and V. Adimurthy, "An analysis of near-circular lunar mapping orbits," *Journal of Earth System Science*, vol. 114, no. 6, pp. 619–626, 2005.